

# Preparation and Characterization of a Solid Acid Catalyst from Macro Fungi Residue for Methyl Palmitate Production

Min Wang,<sup>a</sup> Wei-Wei Wu,<sup>a</sup> Sha-Sha Wang,<sup>a</sup> Xin-Yi Shi,<sup>a</sup> Fu-An Wu,<sup>a,b</sup> and Jun Wang<sup>a,b,\*</sup>

During the process of fungal polysaccharide extraction for health care products and food factories, a large quantity of macro-fungi residues are produced, but most of the residues are abandoned and become environmental pollutants. A solid acid catalyst, prepared by sulfonating carbonized *Phellinus igniarius* residue, was shown to be an efficient and environmentally benign catalyst for the esterification of palmitate acid (PA) and methanol. As a comparison, two types of common biomass catalysts, wheat straws and wood chips, were prepared. In this study, characterizations, including scanning electron microscopy, thermogravimetric analysis, Fourier transform infrared spectrometry, Brunauer-Emmett-Teller assays and elemental analysis, and reaction conditions for the synthesis of methyl palmitate (MP) using solid acid catalysts were investigated. Experiments showed that the solid acid catalyst prepared from *P. igniarius* residue had a higher catalytic activity than the other two catalysts, and the highest yield of MP catalyzed by *P. igniarius* residue solid acid catalyst was 91.5% under the following optimum conditions: molar ratio of methanol/PA of 10:1, reaction temperature of 60 °C, mass ratio of catalyst/substrate of 2%, and a reaction time of 1.5 h. Thus, the use of this catalyst offers a method for producing MP.

*Keywords:* Biomass; Catalyst preparation; Catalyst characterization; Esterification; Heterogeneous catalysis; Macro fungi residue

*Contact information:* a: School of Biotechnology, Jiangsu University of Science and Technology, Zhenjiang 212018, P R China; b: Sericultural Research Institute, Chinese Academy of Agricultural Sciences, Zhenjiang 212018, P R China; \* Corresponding author: wangjun@just.edu.cn

## INTRODUCTION

Acid and base catalysts play vital roles in organic synthesis. Many organic reactions, such as alkylation, isomerization, esterification, cracking, acylation, nitration, and condensation, among others, are accomplished by acid catalysts (Jin *et al.* 2014). Conventionally, these organic reactions have been performed using homogeneous liquid acid catalysts, such as sulfuric acid, phosphoric acid, hydrofluoric acid, and succinic acid (Delhomme *et al.* 2012), among others, especially in biodiesel production. Biodiesel can be produced using acid and base catalysts. Base-catalyzed esterification is most commonly used for the commercial-scale production of biodiesel (Zhang *et al.* 2013). Industrially, sodium hydroxide and potassium hydroxide are typically selected as catalysts because they are relatively inexpensive and active (Yusup and Khan 2010). However, with this conventional method, it is difficult to remove these base catalysts after the reaction, and a large amount of waste water is produced to separate the catalyst from the product (Soares *et al.* 2013). In addition, the use of a homogeneous base catalyst

causes saponification when raw materials contain high contents of free fatty acids and water, creating a serious problem for product separation and ultimately decreasing the yield of fatty acid methyl ester (FAME). Homogeneous acid catalysts, such as  $\text{H}_2\text{SO}_4$ , can simultaneously catalyze esterification and transesterification, and they have a better performance with free fatty acids (FFAs) than base catalysts in the esterification process (Shu *et al.* 2010b). However, the use of liquid acid catalysts has some disadvantages, such as lack of recovery, costly separation of catalysts, equipment corrosion, long reaction time, and serious environmental pollution (Endalew *et al.* 2011). These disadvantages severely limit the applications of liquid acid catalysts in the industry. Because of the advantages of solid acid catalysts, such as high reactivity, lack of corrosion, environmental friendliness (Sani *et al.* 2014), easy handling, low cost, and easy recovery and reuse, numerous efforts have been made to use novel environmentally friendly heterogeneous solid acid catalysts as replacements for traditional homogeneous liquid acid catalysts.

For the catalytic process, the various solid acid catalysts can be divided into two groups, in which one group is composed of commercial solid acid catalysts, including ion-exchange resins and heteropolyacids that have been reported to exhibit excellent catalytic activity in the esterification reactions of free fatty acids. However, the high cost and low heat stability of commercial catalysts greatly hinder their widespread application (Liu *et al.* 2013). Another group is composed of solid acid catalysts prepared in-lab from biomass wastes, which include agricultural and forestry waste and microalgae and macro-fungi residues. These catalysts can be inexpensively and easily produced by the incomplete carbonization of sulfopolycyclic aromatic hydrocarbons or the sulfonation of incompletely carbonized inorganic or organic compounds (Chen and Fang 2011). Solid acid catalysts prepared from the sulfonation of agricultural and forestry waste, including sawdust, bamboo leaves, and wheat straw, can reduce not only the cost of catalysts but also the waste, thus protecting the environment. As reported, solid acid catalysts prepared from the sulfonation of carbonized compounds, such as starch and glucose, can form a rigid carbon material composed of small polycyclic aromatic carbon sheets by carbonization (Zong *et al.* 2007); sulfonating these carbon materials can likely form a highly stable solid with a high density of active sites. These carbon solid acid catalysts also showed high catalytic activity and stability. The microalgae residue-based catalyst reported by Fu *et al.* (2013) showed high catalytic activity and can be regenerated, while its activity can be well-maintained after five cycles. As the main component of the biosphere, macro fungi have been widely used in the food and medicine industries and have wide prospects for application and exploitation. However, no reports have been presented on the preparation of solid acid catalysts from macro-fungi residue resources until now. As a type of typical macro fungi, *Phellinus igniarius* has been increasingly favored because of its considerable nutritional and medicinal value. However, after polysaccharide extraction from *P. igniarius*, the *P. igniarius* residue has generally been discarded or burned, which was a common phenomenon in food factories and pharmaceutical companies. In this study, a novel carbon-based solid acid catalyst derived from *P. igniarius* residue by carbonization and sulfonation was synthesized. For comparative purposes, two types of common biomass catalysts, including wheat straw and wood chips, were prepared.

Solid acid catalysts can be widely used in the chemical industry, such as petroleum, coal chemical processing, pharmaceuticals, fine chemicals, and environmental protection areas (Zheng *et al.* 2013). Generally, esterification between fatty acids and

methanol can be achieved using solid acids as catalysts to produce the corresponding methyl ester, namely biodiesel (Chen *et al.* 2014). Biodiesel, an alternative fuel consisting of fatty acid methyl esters (FAMES) (Shu *et al.* 2010a), is renewable, biodegradable, and non-toxic, and has gained increasing attention in recent years because it is regarded as a promising remedy to counteract negative environmental effects resulting from the overconsumption of non-sustainable fossil fuels (Raita *et al.* 2011; Deshmane *et al.* 2013). Heterogeneous solid acid catalysts, which can be easily and efficiently separated from their products for reuse, are desirable for many applications (Sheikh *et al.* 2013), but most solid acid catalysts reported to date are either expensive or difficult to prepare (Jeong *et al.* 2015). In addition to recyclability and reusability, an ideal solid acid catalyst for biodiesel preparation should have high stability, numerous strong acid sites, a hydrophobic surface, and low cost (Sani *et al.* 2013). As a fine raw material for the preparation of a solid acid, *P. igniarius* residue possesses a regular pore structure, high carbon content, and extensive source properties; thus, it has a great future for applications.

The objective of this study was to characterize the solid acid catalysts prepared by biomass wastes and to synthesize methyl palmitate (MP) from palmitate acid (PA) using the catalysts. In this study, three types of solid acid catalysts were used in the esterification reaction of PA with methanol for MP production. These inexpensive catalysts were prepared by sulfonating carbonized biomass with  $-SO_3H$  functional groups as the active sites. Scanning electron microscopy (SEM), thermo-gravimetric analysis (TG), Fourier transform infrared spectrometry (FTIR), Brunauer-Emmett-Teller (BET) assays, and elemental analysis (EA) were used to characterize the solid acid catalysts. In the present study, using three solid acid catalysts prepared from macro fungi residue and two other types of common biomass, including wheat straws and wood chips, the factors that strongly affect the yield of MP (reaction temperature, catalyst loading, the molar ratio of methanol to PA, and reaction time) were explored. The *P. igniarius* residue solid acid catalyst was found to have higher catalytic activity than the other two catalysts.

## EXPERIMENTAL

### Materials

*P. igniarius* residue, wheat straw, and wood chips were manufactured in our lab. The FAME standards, including methyl heptadecanoate (internal standard) and methyl palmitate, were purchased from Sigma Co. (St. Louis, MO, USA). PA, methanol, sulfuric acid, n-hexane, and all other reagents and solvents were of analytical grade (Sinopharm Chemical Reagent Co., Ltd., Shanghai, China). Water was purified using an Elga Purelab Option-Q purification system (Elga Labwater, High Wycombe, Bucks, UK) and had a minimum resistivity of 18.0 M $\Omega$  cm.

### Catalysts Preparation

*P. igniarius* residue, wheat straw, and wood chip solid acid catalysts were prepared with the following steps. The raw materials, including *P. igniarius* residue, wheat straws, and wood chips, were pyrolyzed in a muffle furnace under  $N_2$  at 400 °C for 10 h. After cooling to room temperature, the resulting carbonized materials were immersed in concentrated sulfuric acid (>98%) overnight. Then, the black precipitates, which were collected by filtration, were placed in a muffle furnace at 150 °C for 15 h.

After cooling to ambient temperature, the precipitates were washed repeatedly with distilled water until the sulfate ions were no longer detected in the wash water. Then, the prepared solid acid catalysts were dried at 60 °C for 48 h in a drying oven, bagged, and placed in a desiccator.

### Catalyst Characterization

SEM images of the samples were recorded on a JSM-6480 scanning electron microscope (JEOL, Japan) equipped with energy dispersive spectroscopy (EDS) operating at 20 kV. The microstructural element components were analyzed. TG was performed under an N<sub>2</sub> atmosphere at a heating rate of 5 °C/min from 30 to 600 °C in flowing air using a TMA403F3 thermal analyzer (NETZSCH, Germany). FTIR spectroscopy was recorded on a TENSOR 27 spectrophotometer (Bruker, Germany). The FTIR spectroscopy measurements were performed by mixing samples into KBr pellets (5 cm<sup>-1</sup> resolution) over the range of 400 to 4000 cm<sup>-1</sup>. The specific surface area and the pore volume were determined by N<sub>2</sub> adsorption-desorption at 77 K using an ASAP 2020 instrument (Micromeritics, USA). Before each measurement, the samples were degassed for 3 h at 200 °C under an N<sub>2</sub> atmosphere. The specific surface area was calculated by the BET method. The total pore volumes were estimated from the amount of N<sub>2</sub> adsorbed at  $P/P_0=0.99$ . The pore size distribution of the catalysts was measured using Barrett-Joyner-Hallenda (BJH) pore size analysis. The elemental compositions of the biomass and the prepared catalyst were determined by EA (Elementar, Germany) using an Elementar Vario EL cube apparatus. The absolute errors were < 0.1% (CHNS) and < 0.2% (O).

### Reaction Procedure

The esterification reaction was performed in a 10-mL screw-cap test tube at a certain temperature with a constant stirring speed of 120 rpm. A stable temperature horizontal shaking bath was used to maintain a certain reaction temperature. The reaction mixture consisted of PA, methanol (the molar ratio of methanol to PA was 10:1), and 2% w/w catalyst. For a typical run, the PA and sulfonated catalyst were added into the reactor, followed by the introduction of methanol at the required temperature. Aliquots (20 µL) were obtained at specified time intervals from the reaction mixture and were diluted using 80 µL of n-hexane for GC analysis. The effects of the molar ratio of methanol to PA (9:1, 10:1, 11:1, 12:1, 13:1), the mass ratio of catalyst to substrate (1, 2, 3, 4, 5%), reaction temperature (50 to 90 °C), and reaction time (0.5, 1, 1.5, 2, 2.5 h) on the MP yield were investigated. All experiments were performed in triplicate.

### MP Standard Curve and GC Analysis

The MP standard curve was drawn with a horizontal axis of the standard MP concentration and a vertical axis of the average area ratio between the analyte and internal standard (Zhang *et al.* 2010). The linear regression equation of the MP standard curve was  $y=1.0167x-0.0944$ , with an R-squared value of 0.9996 and a linear range for the component of 1 to 10 mg/mL. The result indicated that the MP had good linear relativities ( $R^2 = 0.9996$ ) over the range of 1 to 10 mg/mL. Thus, the calibration curve for the MP standard could be used to calculate and analyze the esterification of PA and methanol.

MP content was determined using an Agilent 6820 gas chromatograph equipped with a Supelco capillary column (HP-Innowax, Agilent, 100 m×0.25 mm, i. d. 0.20 µm), a flame ionization detector, and split injection.

The initial oven temperature was 200 °C, which was held for 1 min, subsequently increased to 250 °C at 1.5 °C/min, and then held for 1 min. The injector was set at 250 °C, and the detector was set at 200 °C. Nitrogen was used as the carrier gas at a flow rate of 1 mL/min. The split ratio was 50:1, and the sample size was 1 µL. All of the experiments were performed in triplicate to determine the experimental variability.

The MP yield was calculated according to Eq. (1):

$$\text{MP yield} = \frac{\text{the mass of ME in product}}{\text{initial mass of palmitic acid}} \times 100\% \quad (1)$$

### Kinetic Model

The kinetic model used in this study relied on the following assumptions: (1) the rate of the esterification is kinetically controlled (Zanuttini *et al.* 2014), (2) the reaction temperature is significant relative to the catalyzed rate, (3) the effects of internal diffusion and external diffusion on esterification can be ignored under mixing, and (4) the methanol/PA molar ratio used was sufficiently high for the methanol concentration to remain constant throughout the process, and the reaction system is considered an ideal solution (Su 2013a).

Under these assumptions, the reaction is assumed to be pseudo-homogeneous and follows the first-order pseudo-homogeneous kinetic model. Therefore, the kinetic equation can be expressed as follows (Eq. 2),

$$-\ln(1-x) = kt \quad (2)$$

where  $x$  is the MP yield (%),  $k$  is the apparent reaction rate constant ( $\text{min}^{-1}$ ), and  $t$  is the reaction time (min).

The influence of reaction temperature on the rate constants can be expressed by the Arrhenius model, as follows (Eq. 3):

$$\ln k = \ln k_0 - \frac{E_a}{RT} \quad (3)$$

where  $k_0$  is the pre-exponential factor for the forward reaction,  $E_a$  denotes the activation energy of the forward reaction,  $R$  is the ideal gas constant, and  $T$  is the reaction temperature.

The effect of temperature was investigated to determine the kinetics of esterification in the batch reactor with a catalyst content of 2%. The pre-exponential factors and activation energy can be determined by fitting the rate constant to the Arrhenius equation.

### Statistical Analysis

Triplicate experiments were conducted for each parameter investigated. The standard deviations of the measurements were calculated to test the reliability of the results. The statistical analyses were performed using the ANOVA method. Significant differences ( $p < 0.05$ ) between the means were determined.

## RESULTS AND DISCUSSION

### Characterizations of the Catalyst

The focus of this study was the *P. igniarius* residue biomass solid acid catalyst prepared by carbonization and sulfonation after pyrolysis. In addition, samples of the sawdust biomass solid acid catalyst and wheat straw biomass solid acid catalyst were prepared for comparison. Physical and chemical data for the catalysts are provided below.

#### SEM studies

SEM images (Fig. 1) show the morphology of the three samples before and after treatment. The elements present in the catalyst samples (C, O, and S) from EDS characterization are given in Table 1.

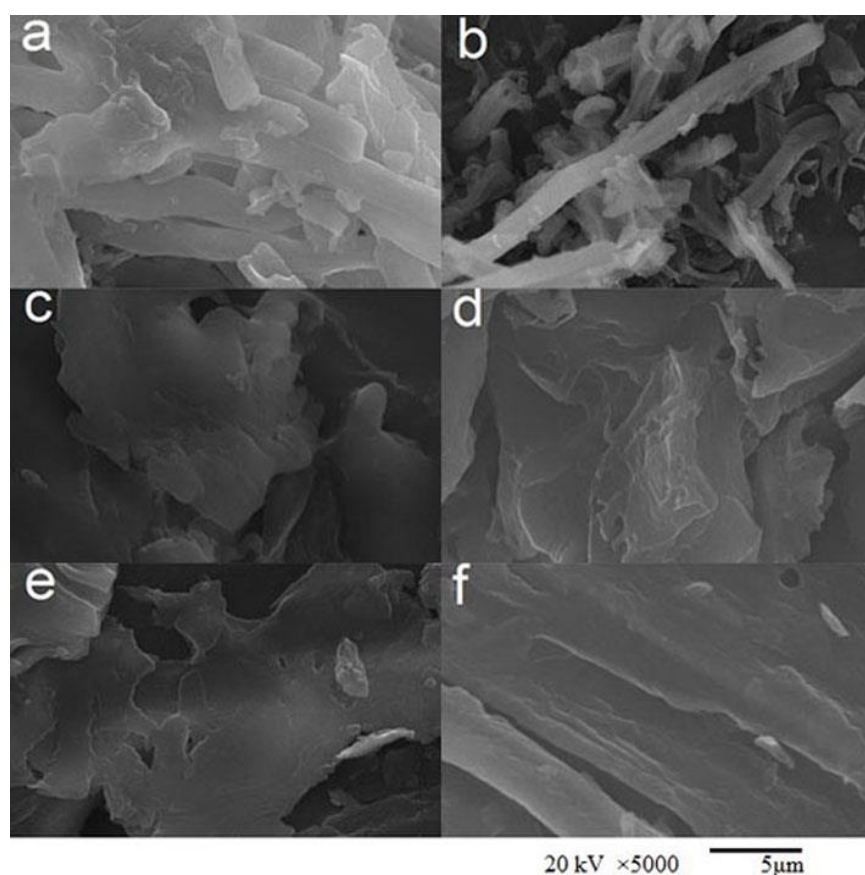


**Fig. 1.** SEM images of (a) *P. igniarius* residue biomass, (b) *P. igniarius* residue biomass solid acid catalyst, (c) sawdust biomass, (d) sawdust biomass solid acid catalyst, (e) wheat straw biomass, and (f) wheat straw biomass solid acid catalyst

**Table 1.** The Elements Present in the Different Solid Acid Catalysts

Catalyst	C%	O%	S%
<i>P. igniarius</i> residue	64.53	32.56	2.91
Sawdust	62.86	34.32	2.82
Wheat straw	68.29	28.67	3.04

Compared with the *P. igniarius* residue biomass, the prepared *P. igniarius* residue biomass solid acid catalyst exhibited a looser irregular sheet structure and irregular particles with a grain size larger than 5  $\mu\text{m}$ , which is similar to the carbon catalyst prepared from microalgae residue reported by Fu *et al.* (2013). Shu *et al.* (2010b) reported obtaining a carbon-based solid acid catalyst using vegetable oil asphalt as the carbon precursor. The obtained vegetable oil asphalt catalyst showed a loose irregular network structure, and several pores with  $\mu\text{m}$  sizes could be observed. The different structures in the *P. igniarius* residue and asphalt catalyst could have resulted from the different main components in these two carbon sources, and it is probable that straight-chain aliphatic hydrocarbon polymers can more easily form pores than ring hydrocarbon polymers when they were incompletely carbonized. Additionally, two other common biomass solid acid catalysts, including the sawdust catalyst and the wheat straw catalyst, consisted of a sheet structure with a smooth surface, which was clearly shown in the SEM images. Furthermore, the morphology showed nonporous characteristics (Rao *et al.* 2011), which was supported by the low BET surface areas of less than 3  $\text{m}^2/\text{g}$ , as determined by nitrogen adsorption measurements. However, the *P. igniarius* residue and catalyst showed several obvious pores, which can be observed in Figs. 1a and b. The larger amounts of pores and larger pore size would increase the accessibility of sulfuric acid into the carbon powder bulk, which would give a higher concentration of covalently bonded carbon with an  $-\text{SO}_3\text{H}$  group. The incorporation of a larger amount of hydrophilic functional groups ( $-\text{SO}_3\text{H}$ ) into the carbon sheet will improve the hydrophilicity of the carbon material; thus, the hydrophilic methanol molecules can more easily penetrate the interior of the carbon bulk and react with hydrophobic reactants (PA) on the interior acid sites of this catalyst.

#### BET studies

The different BET surface areas result in different amounts of acid sites on the exterior or in the interior of the solid acid catalyst (Shu *et al.* 2010b); thus, the BET surface area of the three types of catalysts was measured. The pore volume and size are also important parameters for a porous material in a catalytic application to make biodiesel because this process involves large organic molecules. The physicochemical properties of the three types of catalysts prepared from *P. igniarius* residue, sawdust biomass, and wheat straw biomass are shown in Table 2.

**Table 2.** Textural Properties and Catalytic Activity of Various Solid Acid Catalysts

Catalysts	$S_{\text{BET}}$ ( $\text{m}^2\text{g}^{-1}$ )	$V_{\text{Total}}$ ( $\text{cm}^3\text{g}^{-1}$ )	$\Phi_p$ (nm)	$t$ (h)	$T$ ( $^{\circ}\text{C}$ )	Ester Yield (%)	References
<i>P. igniarius</i>	4.71	0.009	7.35	1.5	60	91.54	This work
Sawdust	15.79	0.004	0.99	1.5	60	65.80	This work
Wheat straw	1.45	-	-	1.5	60	55.90	This work
D-Glucose	4.10	0.440	4.00	3.0	80	76.00	(Lou <i>et al.</i> 2008)
Palygorskite	178	0.364	-	4.0	120	46.12	(Jiang <i>et al.</i> 2014)

The BET surface areas ranged from 15.79 (sawdust) to 1.45 (wheat straw)  $\text{m}^2/\text{g}$ , and the mean pore size ranged from 7.35 (*P. igniarius*) to 0.99 nm (sawdust). It can be observed that the surface area of the carbon-based catalysts decreased with increasing pore size, and it can be concluded that the different carbon sources caused the produced

catalysts to have different pore sizes after they underwent carbonization and sulfonation. The larger pore size would increase the accessibility of sulfuric acid into the carbon powder bulk, which would give a higher concentration of covalently bonded carbon with an  $-\text{SO}_3\text{H}$  group (Shu *et al.* 2010b). The textural study reveals that the sawdust catalyst presents a microporous network, as can be inferred from an average pore size of 0.99 nm, which renders difficult the access of the PA molecules to the sulfonic acid sites located into the micropores. The *P. igniarius* catalyst had the largest pore size (7.35 nm). The low surface area ( $4.71 \text{ m}^2/\text{g}$ ) of the *P. igniarius* catalyst may indicate that most of the  $-\text{SO}_3\text{H}$  groups were in the interior of this catalyst. If the pore size of the catalyst is small, then the entry of a bulky organic molecule reactant will be obstructed (Lou *et al.* 2008). Because the average pore size of the sulfonated *P. igniarius* residue was relatively large (7.35 nm), the reactants could easily diffuse into the interior of the catalyst, which allowed the reactants to come into contact with more acid sites, resulting in better activity for the *P. igniarius* catalyst. Table 1 shows comparative textural properties and catalytic activity of various solid acid catalysts. Jiang *et al.* (2014) reported that the BET surface area of the palygorskite catalyst they obtained was 178 nm, which was larger than that of the *P. igniarius* catalyst. However, the ester yield of the palygorskite catalyst was much less than that of the *P. igniarius* catalyst.

#### TG studies

Figure 2 shows the TG curves for sulfonated and raw biomass in air. Thermogravimetric analysis showed the stability of the acid site for different carbon-based catalysts (Corro *et al.* 2014).

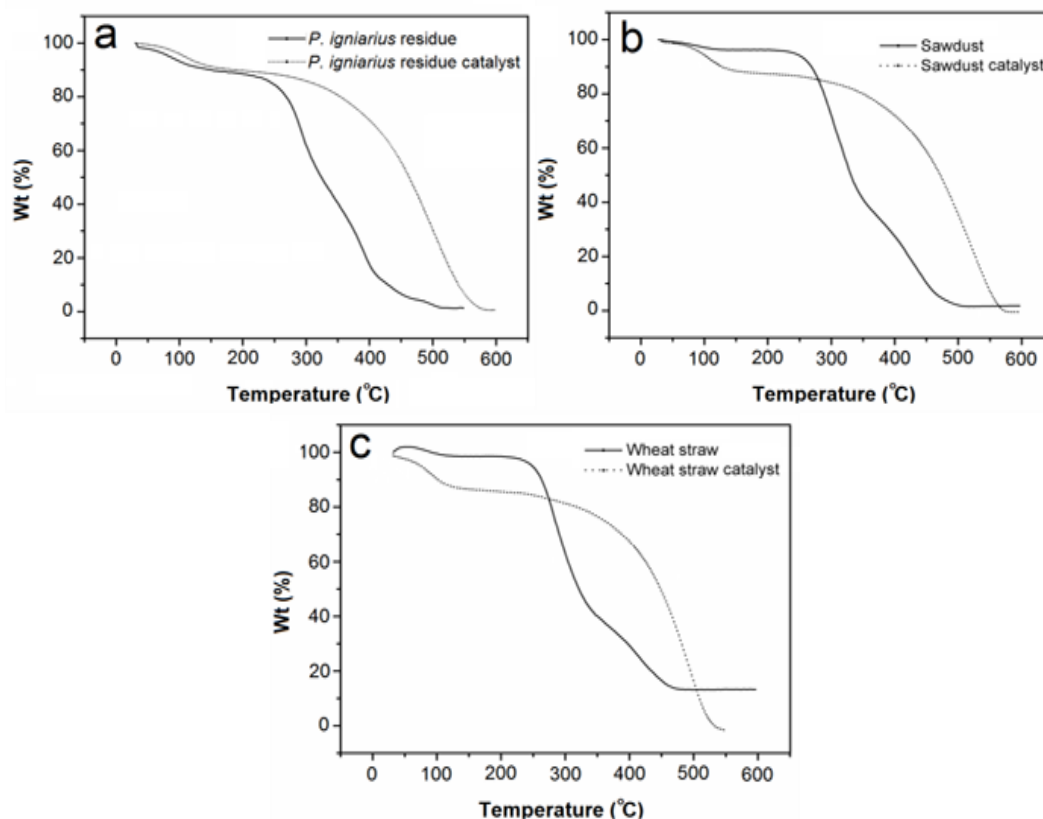


**Fig. 2.** TG of (a) *P. igniarius* residue biomass and *P. igniarius* residue biomass solid acid catalyst; (b) sawdust biomass and sawdust biomass solid acid catalyst, and wheat straw biomass; and (c) wheat straw biomass solid acid catalyst

As indicated in TG, a constant mass was achieved above 580 °C for the *P. igniarius* solid acid catalyst. The curve reveals that decomposition started at approximately 50 °C with a slight weight loss, corresponding to the volatilization of surface adsorbed water and small molecules. The TG curve of the *P. igniarius* catalyst tended to be relatively constant over a temperature range of 150 to 350 °C, while the TG curve of the *P. igniarius* residue tended to be relatively constant over a temperature range of 150 to 250 °C. This result indicated that the solid acid catalyst lost only a minor amount of weight and showed a higher stability than the raw *P. igniarius* residue. The next stage of *P. igniarius* catalysis began at 350 °C and was completed at 580 °C with a rapid weight loss due to the pyrolysis of organic groups, while the raw *P. igniarius* residue showed a rapid weight loss up to 510 °C. This peak is exothermic because of the concomitant oxidation reaction occurring with decomposition (Rashtizadeh *et al.* 2014). In this decreasing process, the internal structure of the *P. igniarius* solid acid catalyst changed, leading to a decrease in catalytic activity. The sawdust biomass solid acid catalyst and the wheat straw biomass solid acid catalyst showed similar thermal behaviors over a temperature range of 100 to 550 °C. However, the wheat straw biomass solid acid catalyst demonstrated a faster weight loss rate.

#### FT-IR studies

Figure 3 shows FT-IR spectra for sulfonated and raw carbon material. The absorption bands at approximately 1612  $\text{cm}^{-1}$  and 1386  $\text{cm}^{-1}$  for the catalyst and its precursor, respectively, were assigned to the aromatic-like C=C stretching mode in the polyaromatic sketch, which can be clearly observed in the sulfonated *P. igniarius* residue and wheat straw (Figs. 3a and b).

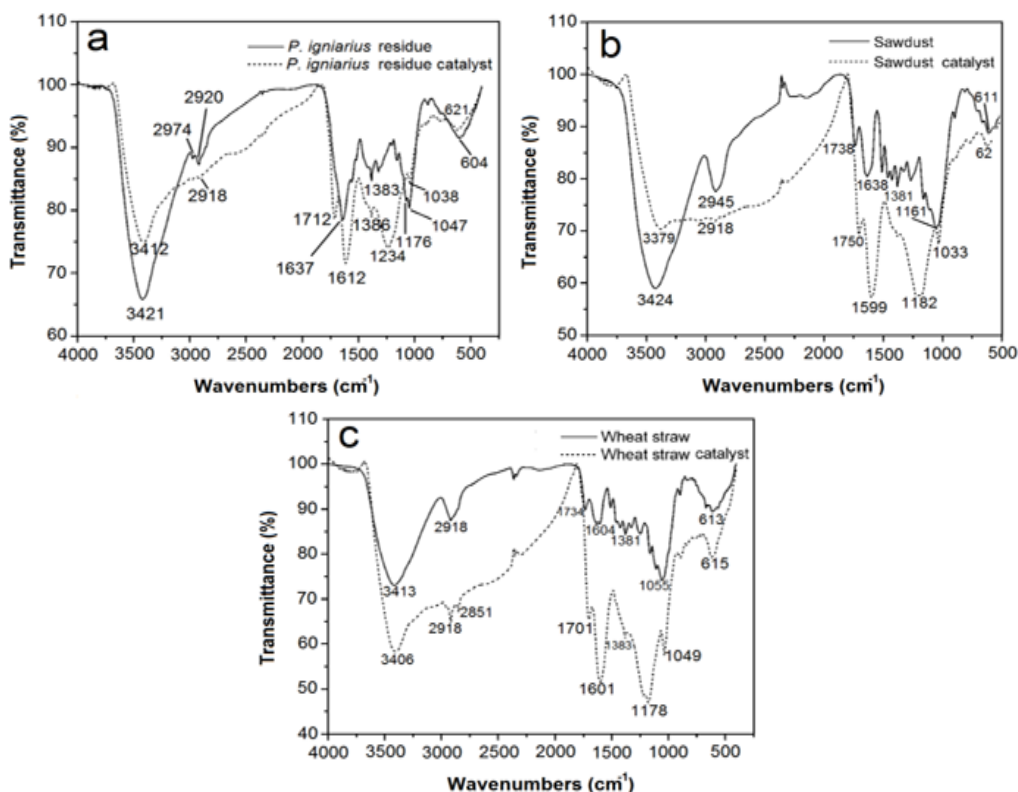


**Fig. 3.** FT-IR spectra of (a) *P. igniarius* residue biomass and corresponding catalyst; (b) sawdust biomass and its catalyst; (c) wheat straw biomass and the corresponding solid acid catalyst

The band at  $3421\text{ cm}^{-1}$  in the *P. igniarius* residue and the band at  $3412\text{ cm}^{-1}$  in the *P. igniarius* catalyst were assigned to the  $\text{-OH}$  stretching modes of the  $\text{-COOH}$  and phenolic  $\text{OH}$  groups, revealing the presence of the  $\text{-OH}$  group in pre- and post-sulfonation. Similarly, the bands at  $3406\text{ cm}^{-1}$  and  $3413\text{ cm}^{-1}$  for the wheat straw catalyst and its precursor and the bands at  $3379\text{ cm}^{-1}$  and  $3424\text{ cm}^{-1}$  for the sawdust catalyst and its precursor, respectively, were assigned to the  $\text{-OH}$  stretching modes. The band at  $1712\text{ cm}^{-1}$  in the *P. igniarius* catalyst was assigned to the  $\text{C=O}$  stretching mode of the  $\text{-COOH}$  group. The vibration bands located at  $1038\text{ cm}^{-1}$  ( $\text{-SO}_2\text{-}$  symmetric stretching) and  $1234\text{ cm}^{-1}$  ( $\text{-SO}_2\text{-}$  asymmetric stretching) are clearly visible in the sulfonated *P. igniarius* residue FT-IR spectrum, demonstrating the presence of the  $\text{-SO}_3\text{H}$  group. Similarly, the bands at approximately  $1040\text{ cm}^{-1}$  and  $1180\text{ cm}^{-1}$  for sulfonated wheat straw and sawdust were evidence that the as-prepared catalysts had been functionalized with catalytic sites ( $\text{-SO}_3\text{H}$ ) on the surface. All of the correlation bands produced by chemical bonds in the carboxyl group were weakened after carbonization and sulfonation (Figs. 3a and c), which indicated that the side chain groups were cleaved in the experiment (Jiang *et al.* 2014). From the previous analysis, it is possible to qualitatively conclude that there were many  $\text{-SO}_3\text{H}$  groups in the sulfonated *P. igniarius* residue.

#### EA studies

As shown in the elemental analysis (Table 3), the S contents in the *P. igniarius* residue biomass were 0.12% and 2.95% before and after sulfonation, respectively, indicating the successful introduction of  $\text{-SO}_3\text{H}$  into the aromatic carbon rings *via* sulfonation. Elementary analysis (EA) showed that the pre- and post-sulfonation had clearly different compositions. Also, the S content of EA data was generally in agreement with EDS analysis during SEM study. Since all sulfur in the carbon materials was expected to be in the form of  $\text{-SO}_3\text{H}$  groups, the densities of these groups was estimated based on the S content in the catalyst compositions determined by EA (Liu *et al.* 2013). The  $\text{-SO}_3\text{H}$  density of *P. igniarius* catalyst, sawdust catalyst and wheat straw catalyst were 0.92, 0.90, and 0.96 mmol/g, respectively.

**Table 3.** Elemental Analysis of Different Biomass and Solid Acid Catalysts

Samples	C%	H%	N%	S%
<i>P. igniarius</i> residue	48.62	5.11	1.11	0.12
<i>P. igniarius</i> catalyst	57.77	2.54	3.09	2.95
Sawdust biomass	46.62	6.577	1.131	0.09
Sawdust catalyst	57.40	3.568	1.048	2.87
Wheat straw biomass	42.62	6.434	1.004	0.14
Wheat straw catalyst	59.99	3.553	1.996	3.05

#### Comparison of Three Types of Solid Acid Catalysts

It is of particular interest to compare the catalyst activities of the carbon-based catalysts with those of concentrated  $\text{H}_2\text{SO}_4$  (>96%). The esterification activities were evaluated through the esterification of PA with methanol (mass ratio of methanol to PA of 10:1) at  $60\text{ }^\circ\text{C}$ . Figure 4 shows the results of a 2% content of all tested catalysts. After 1.5 h, the three corresponding catalysts prepared from the *P. igniarius* residue (macro fungi residue) and the two other types of common biomass (wheat straws and wood chips) gave yields of 91.54%, 55.90%, and 65.80%, respectively.

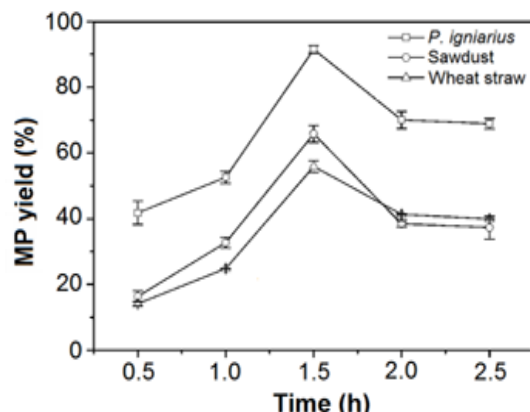


**Fig. 4.** Time-dependent curves of MP formation catalyzed by various carbon-based catalysts prepared from different starting materials (*P. igniarius* residue, sawdust, and wheat straw). Reaction conditions: a molar ratio of methanol to PA of 10:1, a catalyst content of 2%, and a reaction temperature of 60 °C.

Compared with other studies, such as those using D-glucose and palygorskite solid acid catalysts, the *P. igniarius* residue catalyst exhibited a high activity within a short time at a low temperature (Table 1). It is obvious that different raw materials exerted a significant effect on the catalytic activity of the resulting catalyst samples (Xu *et al.* 2014). The time-dependent curves of the MP yield, as depicted in Fig. 4, clearly indicate that the *P. igniarius* residue catalyst was much more active than the other catalysts, achieving the maximum yield of 91.54% within only 1.5 h.

### Effect of Several Factors on the MP Yield

Figure 5a shows the effect of the molar ratio of methanol to PA on the yield of MP in esterification. The esterification reaction between PA and methanol follows a reversible path (Abbaszaadeh *et al.* 2012). A higher equilibrium conversion can be obtained only if the backward reaction is minimized. There are two methods for reducing the rate of the backward reaction, as follows: a) continuously remove one of the undesired products, *i.e.*, water in the present case, or b) use one of the reactants in excess (in this case, methanol) (Wang *et al.* 2013). In the present system, it was difficult to remove water because the employed system was closed. Thus, the option of using excess methanol was employed in the present study. The amount of methanol must be in excess to force the reaction towards the formation of MP. It is shown in Fig. 5a that the yield of MP increased as the molar ratio of methanol to PA was increased from 9 to 10. However, with the increase of the molar ratio of methanol to PA from 10 to 13, the yield of MP decreased, which can be explained as follows. Firstly, the hydrophilic property of this carbon catalyst was improved due to the hydrophilic functional groups ( $-\text{SO}_3\text{H}$ ) bonded to its carbon sheet. The increased molar ratio accelerates the esterification and produces more water. Unfortunately, an excessive amount of water greatly reduces the acidic hydroxyl groups ( $-\text{OH}$ ) because the groups become hydrated (Park *et al.* 2010). Secondly, when the ratio of methanol to PA was too high, the large excess of methanol caused flooding of the active sites. Therefore, the increased molar ratio hindered the conversion of FFA protonation at the active sites. From this analysis, it can be deduced that the molar ratio of methanol to PA cannot be too high. Thus, a molar ratio of methanol to PA of 10 is recommended.

Figure 5b shows the effect of catalyst loading on the yield of MP in esterification. The amount of catalyst also affected the esterification reaction between PA and methanol (Liu *et al.* 2014). The sulfonated macro fungi residue catalyst was used to study the effect of catalyst loading (1, 2, 3, 4, and 5%) on the yield of MP, with the other reaction conditions held constant. The results are shown in Fig. 5b, which indicates that there was a significant increase in the yield of MP as the mass ratio of catalyst to substrate increased from 1 to 2% under identical conditions. However, with the increase of the catalyst loading from 2 to 5%, the MP yield decreased. Several researchers have observed a similar phenomenon (Peng *et al.* 2008), which can be explained as follows. At a catalyst loading of 5%, the yield of MP was significantly lower because the higher catalyst loading accelerates the esterification of PA, and more water is formed in a shorter time. Excess water deactivates the acidic hydroxyl groups ( $-OH$ ) because the hydration of these groups occurs when water is present (Zhang *et al.* 2014). The optimum catalyst loading was chosen as 2% for further studies.

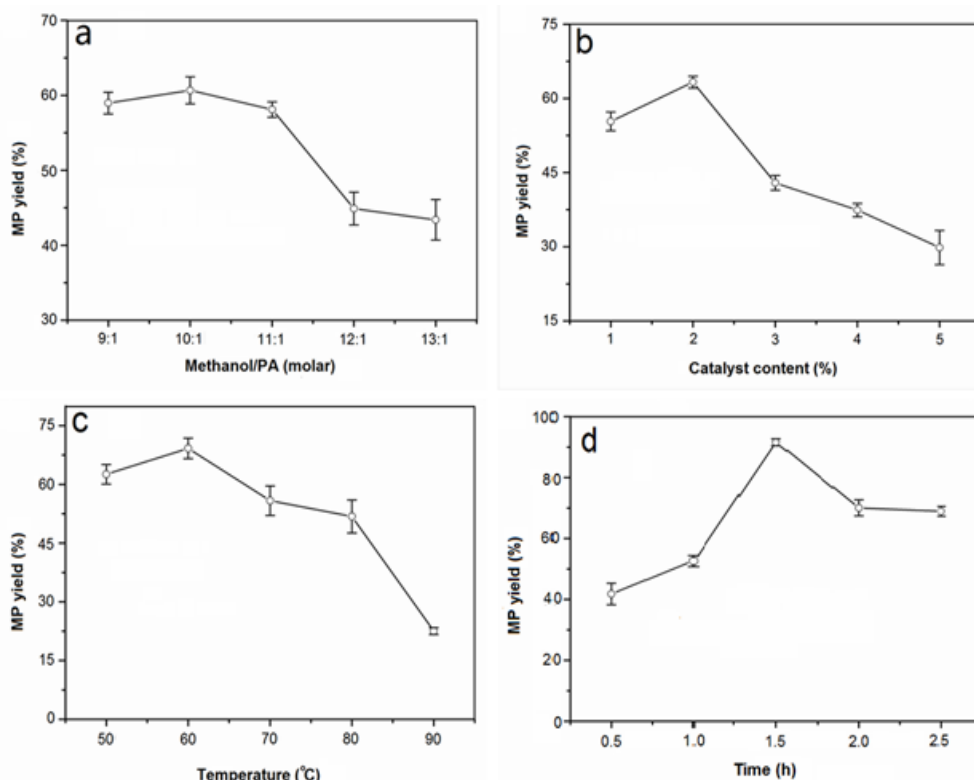


**Fig. 5.** Effects of (a) molar ratio of methanol to PA; (b) catalyst content; (c) reaction temperature; and (d) reaction time on the yield of MP catalyzed by *P. igniarius* residue biomass solid acid catalyst. Reaction conditions: (a) To assess the effects of the molar ratio of methanol to PA on the yield of MP, the molar ratio of methanol to PA was increased from 9:1 to 13:1, the mass ratio of catalyst to substrate was 2%, the speed of agitation was 60 rpm, the temperature was 70 °C, and the reaction time was 2 h. (b) To assess the effect of the catalyst content on the yield of MP, the mass ratio of catalyst to substrate was increased from 1% to 5%, the molar ratio of methanol to PA was 10:1, the speed of agitation was 60 rpm, the temperature was 70 °C, and the reaction time was 2 h. (c) To assess the effect of the reaction temperature on the yield of MP, the reaction temperature was increased from 50 °C to 90 °C, the molar ratio of methanol to PA was 10:1, the mass ratio of catalyst to substrate was 2%, the speed of agitation was 60 rpm, and the reaction time was 2 h. (d) To assess the effect of reaction time on yield of MP, the reaction time was increased from 0.5 h to 2.5 h, the molar ratio of methanol to PA was 10:1, the mass ratio of catalyst to substrate was 2%, the speed of agitation was 60 rpm, and the temperature was 60 °C.

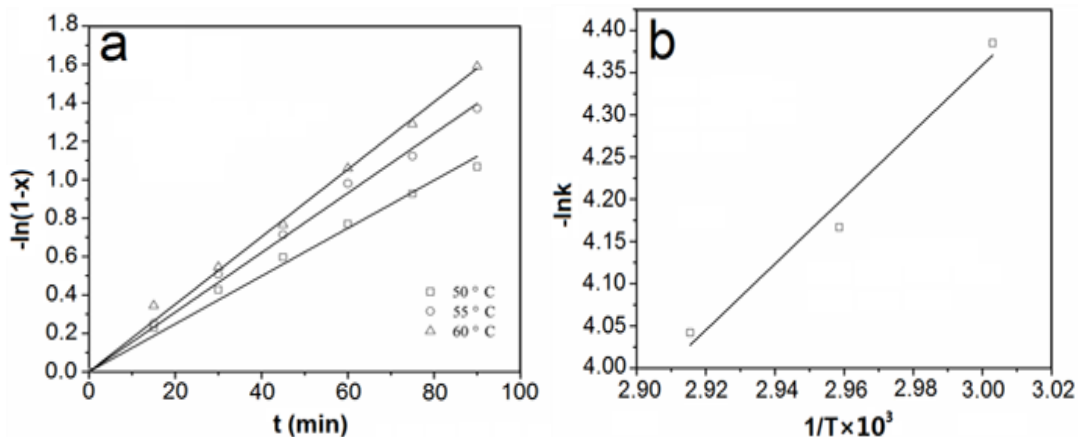
Figure 5c shows the yield of MP under different reaction temperature conditions with the esterification of PA and methanol. The reaction temperature is one of the most important parameters affecting MP yield during the esterification process (Narkhede *et al.* 2014). Six different temperatures were selected over the range of 50 to 90 °C. The other reaction conditions were a molar ratio of methanol to PA 10:1 and a catalyst concentration of 2%. From Fig. 5c, it can be observed that the yield of methyl ester markedly increased (from 62.6% to 69.2%) as the reaction temperature was increased from 50 to 60 °C. A higher temperature results in an increase in the reaction rate and the equilibrium constant for an endothermic reaction. With a further increase to 70 °C, the yield of MP decreased to 55.9%. These results indicate that higher temperatures could activate substrate molecules, reduce the viscosity of the reaction mixture, and lead to a higher reaction rate (Narkhede *et al.* 2014). However, a temperature that is too high could increase the water content, accelerate the esterification and produce more water. Furthermore, the presented water leads to the decrease of MP. Therefore, a temperature of 60 °C was used in subsequent optimization experiments.

Figure 5d shows the effect of reaction time on the yield of MP in esterification. The reaction time also affects the conversion efficiency of the process. The effect of reaction time (0.5, 1, 1.5, 2, and 2.5 h) on the yield of MP was studied. The reaction occurred at 60 °C with a molar ratio of methanol to PA of 10:1 and a catalyst loading of 2%. With an increase in time from 0.5 to 1.5 h, the yield of MP increased markedly from 42% to 92%. However, when the reaction time was further increased to 2.5 h, the yield of MP significantly decreased, which could be explained as follows. Excess water was formed as the reaction progressed, which deactivated the acidic hydroxyl groups (–OH) because these groups are hydrated when water is present (Park *et al.* 2010). Thus, the reaction time should be 1.5 h.

### Reaction Rate Constants and Activation Energy

The reaction rate constant ( $k$ ) can be estimated by a linear equation defined as Eq. 2. Figure 6a shows the correlation between  $-\ln(1-x)$  and  $t$  under all experimental conditions. As observed, a straight line with a negligible intercept is a clear indication that the proposed model is valid. The experimental data were correlated with a first-order pseudo-homogeneous kinetic model. Hence, the reaction rate constant  $k$  can be calculated from the slope of each straight line. Figure 6b also shows that this reaction is endothermic because the rate constant increased with the reaction temperature (Berrios *et al.* 2007). The kinetic rate constants were similarly obtained at 50, 55, and 60 °C with a 2% catalyst concentration. The apparent reaction rate constants ( $k_1$ ,  $k_2$ , and  $k_3$ ) for the 2% catalyst concentration at 50, 55, and 60 °C were 0.01246, 0.0155, and 0.01756  $\text{min}^{-1}$  with correlation coefficients ( $R^2$ ) of 0.9966, 0.9983, and 0.9985, respectively.

The effect of temperature on the reaction rate constants was determined by fitting  $k_1$ ,  $k_2$ , and  $k_3$  to the Arrhenius equation. As shown in Fig. 6b, the higher linear correlation coefficients (0.96) indicated that the plot was represented by a straight line (Rani *et al.* 2013). Hence, the Arrhenius model parameters were obtained from the slope and intercept of the straight line, and the activation energy and pre-exponential factor of this reaction were calculated as 32.61 kJ/mol and  $1.65 \times 10^3 \text{ min}^{-1}$ , respectively. These high values for the activation energy indicate that the reaction is temperature-sensitive (Su 2013a) and confirm the assumption of a kinetically controlled reaction.



**Fig. 6.** Determination of (a) the kinetic constants using Eq. (2) at 50, 55, and 60 °C. Effect of temperature on (b) the reaction rate constant at 2% catalyst concentration and 13:1 methanol/PA molar ratio.

### Reusability and Service Life of *P. igniarius* Solid Acid Catalyst

In addition to the simple catalyst removal step and being environmentally friendly, another main advantage of the solid acid catalyst is its reusability (Kouzu *et al.* 2011). The efficiency of the solid acid catalyst depends on its reusability. To evaluate its reusability, a series of esterification reaction cycles was performed with the recovered *P. igniarius* residue catalyst. Methanol was used to wash the catalyst, which was separated by filtration. Then, the catalysts were dried and used to perform esterification (Su 2013b). The data for the reusability of the catalyst are presented in Fig. 7. From the fresh use run to the completion of the sixth reuse run, all of the MP yields were greater than 50%. The experimental results indicate that the sulfonated *P. igniarius* residue (the macro fungi residue) is a stable catalyst and is suitable for intermediate-term use.

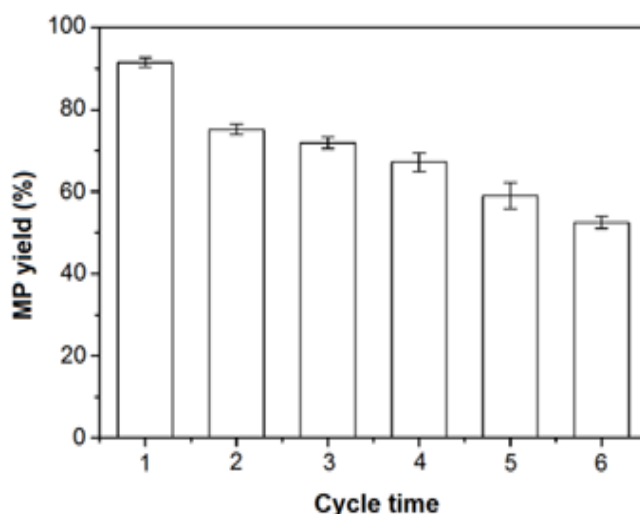


**Fig. 7.** Reusability and service life of *P. igniarius* residue solid acid catalyst. Reaction conditions: a molar ratio of methanol to PA of 10:1, a catalyst content of 2%, a reaction temperature of 60 °C, and a reaction time of 1.5 h

## CONCLUSIONS

1. The solid acid catalyst of *P. igniarius* residue was firstly applied to the production of methyl palmitate (MP).
2. A yield of 91.54% of MP was obtained by the following optimum conditions: reaction temperature of 60 °C, molar ratio of methanol to PA of 10:1, catalyst loading of 2%, and reaction time of 1.5 h.
3. A high catalytic activity, an intermediate catalyst life, and environmentally friendly properties of the *P. igniarius* residue solid acid catalyst were achieved for the MP synthesis, tended to be an efficient catalyst for the biodiesel production.

## ACKNOWLEDGMENTS

This study was financially supported by the Science and Technology Support Program of the Jiangsu Province of China (BE2013405), the Qing Lan Project of the Jiangsu Province of China (2014), the Modern Agro-industry Technology Research System of China (CARS-22), and the Shen Lan Young scholars program of Jiangsu University of Science and Technology (2015). The authors have declared no conflicts of interest.

## REFERENCES CITED

- Abbaszaadeh, A., Ghobadian, B., Omidkhah, M. R., and Najafi, G. (2012). "Current biodiesel production technologies: A comparative review," *Energ. Convers. Manage.* 63, 138-148. DOI: 10.1016/j.enconman.2012.02.027
- Berrios, M., Siles, J., Martín, M. A., and Martín, A. (2007). "A kinetic study of the esterification of free fatty acids (FFA) in sunflower oil," *Fuel* 86(15), 2383-2388. DOI: 10.1016/j.fuel.2007.02.002
- Chen, G., and Fang, B. (2011). "Preparation of solid acid catalyst from glucose–starch mixture for biodiesel production," *Bioresource Technol.* 102(3), 2635-2640. DOI: 10.1016/j.biortech.2010.10.099
- Chen, S., Lao-ubol, S., Mochizuki, T., Abe, Y., Toba, M., and Yoshimura, Y. (2014). "Production of *Jatropha* biodiesel fuel over sulfonic acid-based solid acids," *Bioresource Technol.* 157, 346-350. DOI: 10.1016/j.biortech.2014.01.097
- Corro, G., Bañuelos, F., Vidal, E., and Cebada, S. (2014). "Measurements of surface acidity of solid catalysts for free fatty acids esterification in *Jatropha curcas* crude oil for biodiesel production," *Fuel* 115(0), 625-628. DOI: 10.1016/j.fuel.2013.07.060
- Delhomme, C., Goh, S. L. M., Kühn, F. E., and Weuster-Botz, D. (2012). "Esterification of bio-based succinic acid in biphasic systems: Comparison of chemical and biological catalysts," *J. Mol. Catal. B-Enzym.* 80, 39-47. DOI: 10.1016/j.molcatb.2012.03.010
- Deshmane, C. A., Wright, M. W., Lachgar, A., Rohlfing, M., Liu, Z., Le, J., and Hanson, B. E. (2013). "A comparative study of solid carbon acid catalysts for the esterification of free fatty acids for biodiesel production. Evidence for the leaching of colloidal carbon," *Bioresource Technol.* 147(0), 597-604. DOI: 10.1016/j.biortech.2013.08.073

- Endalew, A. K., Kiros, Y., and Zanzi, R. (2011). "Heterogeneous catalysis for biodiesel production from *Jatropha curcas* oil (JCO)," *Energy* 36(5), 2693-2700. DOI: 10.1016/j.energy.2011.02.010
- Fu, X., Li, D., Chen, J., Zhang, Y., Huang, W., Zhu, Y., Yang, J., and Zhang, C. (2013). "A microalgae residue based carbon solid acid catalyst for biodiesel production," *Bioresource Technol.* 146(0), 767-770. DOI: 10.1016/j.biortech.2013.07.117
- Jeong, G., Kim, S., and Park, D. (2015). "Application of solid-acid catalyst and marine macro-algae *Gracilaria verrucosa* to production of fermentable sugars," *Bioresource Technol.* 181(0), 1-6. DOI: 10.1016/j.biortech.2015.01.038
- Jiang, J., Xu, Y., Duanmu, C., Gu, X., and Chen, J. (2014). "Preparation and catalytic properties of sulfonated carbon-palygorskite solid acid catalyst," *Appl. Clay Sci.* 95(0), 260-264. DOI: 10.1016/j.clay.2014.04.020
- Jin, B., Duan, P., Xu, Y., Wang, B., Wang, F., and Zhang, L. (2014). "Lewis acid-catalyzed in situ transesterification/esterification of microalgae in supercritical ethanol," *Bioresource Technol.* 162(0), 341-349. DOI: 10.1016/j.biortech.2014.03.157
- Kouzu, M., Nakagaito, A., and Hidaka, J. (2011). "Pre-esterification of FFA in plant oil transesterified into biodiesel with the help of solid acid catalysis of sulfonated cation-exchange resin," *Appl. Catal. A-Gen.* 405(1-2), 36-44. DOI: 10.1016/j.apcata.2011.07.026
- Liu, T., Li, Z., Li, W., Shi, C., and Wang, Y. (2013). "Preparation and characterization of biomass carbon-based solid acid catalyst for the esterification of oleic acid with methanol," *Bioresource Technol.* 133(0), 618-621. DOI: 10.1016/j.biortech.2013.01.163
- Liu, W., Yin, P., Zhang, J., Tang, Q., and Qu, R. (2014). "Biodiesel production from esterification of free fatty acid over PA/NaY solid catalyst," *Energ. Convers. Manage.* 82(0), 83-91. DOI: 10.1016/j.enconman.2014.02.062
- Lou, W., Zong, M., and Duan, Z. (2008). "Efficient production of biodiesel from high free fatty acid-containing waste oils using various carbohydrate-derived solid acid catalysts," *Bioresource Technol.* 99(18), 8752-8758. DOI: 10.1016/j.biortech.2008.04.038
- Narkhede, N., Brahmkhatri, V., and Patel, A. (2014). "Efficient synthesis of biodiesel from waste cooking oil using solid acid catalyst comprising 12-tungstosilicic acid and SBA-15," *Fuel* 135, 253-261. DOI: 10.1016/j.fuel.2014.06.062
- Park, J., Wang, Z., Kim, D., and Lee, J. (2010). "Effects of water on the esterification of free fatty acids by acid catalysts," *Renew. Energ.* 35(3), 614-618. DOI: 10.1016/j.renene.2009.08.007
- Peng, B., Shu, Q., Wang, J., Wang, G., Wang, D., and Han, M. (2008). "Biodiesel production from waste oil feedstocks by solid acid catalysis," *Process Saf. Environ.* 86(6), 441-447. DOI: 10.1016/j.psep.2008.05.003
- Raita, M., Laothanachareon, T., Champreda, V., and Laosiripojana, N. (2011). "Biocatalytic esterification of palm oil fatty acids for biodiesel production using glycine-based cross-linked protein coated microcrystalline lipase," *J. Mol. Catal B-Enzym.* 73(1-4), 74-79. DOI: 10.1016/j.molcatb.2011.07.020
- Rani, K., Kumar, T. P., Neeharika, T., Satyavathi, B., and Prasad, R. (2013). "Kinetic studies on the esterification of free fatty acids in *jatropha* oil," *Eur. J. Lipid Sci. Tech.* 115(6), 691-697.

- Rao, B. V. S. K., Chandra Mouli, K., Rambabu, N., Dalai, A. K., and Prasad, R. B. N. (2011). "Carbon-based solid acid catalyst from de-oiled canola meal for biodiesel production," *Catal. Commun.* 14(1), 20-26. DOI: 10.1016/j.catcom.2011.07.011
- Rashtizadeh, E., Farzaneh, F., and Talebpour, Z. (2014). "Synthesis and characterization of Sr3Al2O6 nanocomposite as catalyst for biodiesel production," *Bioresource Technol.* 154(0), 32-37. DOI: 10.1016/j.biortech.2013.12.014
- Sani, Y. M., Daud, W. M. A. W., and Abdul Aziz, A. R. (2013). "Solid acid-catalyzed biodiesel production from microalgal oil - The dual advantage," *J. Environ. Chem. Eng.* 1(3), 113-121. DOI: 10.1016/j.jece.2013.04.006
- Sani, Y. M., Daud, W. M. A. W., and Abdul Aziz, A. R. (2014). "Activity of solid acid catalysts for biodiesel production: A critical review," *Appl. Catal. A-Gen.* 470, 140-161. DOI: 10.1016/j.apcata.2013.10.052
- Sheikh, R., Choi, M., Im, J., and Park, Y. (2013). "Study on the solid acid catalysts in biodiesel production from high acid value oil," *J. Ind. Eng. Chem.* 19(4), 1413-1419. DOI: 10.1016/j.jiec.2013.01.005
- Shu, Q., Gao, J., Nawaz, Z., Liao, Y., Wang, D., and Wang, J. (2010a). "Synthesis of biodiesel from waste vegetable oil with large amounts of free fatty acids using a carbon-based solid acid catalyst," *Appl. Energ.* 87(8), 2589-2596. DOI: 10.1016/j.apenergy.2010.03.024
- Shu, Q., Nawaz, Z., Gao, J., Liao, Y., Zhang, Q., Wang, D., and Wang, J. (2010b). "Synthesis of biodiesel from a model waste oil feedstock using a carbon-based solid acid catalyst: Reaction and separation," *Bioresource Technol.* 101(14), 5374-5384. DOI: 10.1016/j.biortech.2010.02.050
- Soares, D., Pinto, A. F., Gon alves, A. G., Mitchell, D. A., and Krieger, N. (2013). "Biodiesel production from soybean soapstock acid oil by hydrolysis in subcritical water followed by lipase-catalyzed esterification using a fermented solid in a packed-bed reactor," *Biochem. Eng. J.* 81, 15-23. DOI: 10.1016/j.bej.2013.09.017
- Su, C. (2013a). "Kinetic study of free fatty acid esterification reaction catalyzed by recoverable and reusable hydrochloric acid," *Bioresource Technol.* 130, 522-528. DOI: 10.1016/j.biortech.2012.12.090
- Su, C. (2013b). "Recoverable and reusable hydrochloric acid used as a homogeneous catalyst for biodiesel production," *Appl. Energ.* 104, 503-509. DOI: 10.1016/j.apenergy.2012.11.026
- Wang, J., Gu, S., Pang, N., Wang, F., and Wu, F. (2013). "A study of esterification of caffeic acid with methanol using *p*-toluenesulfonic acid as a catalyst," *J. Serb. Chem. Soc.* 78(7), 1023-1034.
- Xu, W., Gao, L., Wang, S., and Xiao, G. (2014). "Biodiesel production in a membrane reactor using MCM-41 supported solid acid catalyst," *Bioresource Technol.* 159, 286-291. DOI: 10.1016/j.biortech.2014.03.004
- Yusup, S., and Khan, M. A. (2010). "Base catalyzed transesterification of acid treated vegetable oil blend for biodiesel production," *Biomass Bioenerg.* 34(10), 1500-1504. DOI: 10.1016/j.biombioe.2010.04.027
- Zanuttini, M. S., Pisarello, M. L., and Querini, C. A. (2014). "Butia Yatay coconut oil: Process development for biodiesel production and kinetics of esterification with ethanol," *Energ. Convers. Manage.* 85, 407-416. DOI: 10.1016/j.enconman.2014.05.080

- Zhang, J., Chen, S., Yang, R., and Yan, Y. (2010). "Biodiesel production from vegetable oil using heterogenous acid and alkali catalyst," *Fuel* 89(10), 2939-2944. DOI: 10.1016/j.fuel.2010.05.009
- Zhang, P., Han, Q., Fan, M., and Jiang, P. (2014). "A novel waste water scale-derived solid base catalyst for biodiesel production," *Fuel* 124, 66-72. DOI: 10.1016/j.fuel.2014.01.091
- Zhang, Y., Wong, W., and Yung, K. (2013). "One-step production of biodiesel from rice bran oil catalyzed by chlorosulfonic acid modified zirconia via simultaneous esterification and transesterification," *Bioresour Technol.* 147, 59-64. DOI: 10.1016/j.biortech.2013.07.152
- Zheng, A., Huang, S., Wang, Q., Zhang, H., Deng, F., and Liu, S. (2013). "Progress in development and application of solid-state NMR for solid acid catalysis," *Chinese J. Catal.* 34(3), 436-491. DOI: 10.1016/S1872-2067(12)60528-2
- Zong, M., Duan, Z., Lou, W., Smith, T. J., and Wu, H. (2007). "Preparation of a sugar catalyst and its use for highly efficient production of biodiesel," *Green Chem.* 9(5), 434-437.

Article submitted: April 20, 2015; Peer review completed: June 29, 2015; Revised version received: July 18, 2015; Accepted: July 19, 2015; Published: July 27, 2015.  
DOI: 10.15376/biores.10.3.5691-5708